Nuclear Theory'25
ed. S. Dimitrova, Heron Press, Sofia, 2006

Dynamical Symmetries Reflected in Realistic Interactions

K. D. Sviratcheva[1], **J. P. Draayer**[1], **J. P. Vary**[2]

[1]Department of Physics and Astronomy, Louisiana State University, Baton Rouge, LA 70803, USA

[2]Department of Physics and Astronomy, Iowa State University, Ames, IA 50011, USA,
Lawrence Livermore National Laboratory, L-414, 7000 East Avenue, Livermore, California, 94551, USA, and
Stanford Linear Accelerator Center, MS81, 2575 Sand Hill Road, Menlo Park, California, 94025, USA

Abstract.

Realistic nucleon-nucleon (NN) interactions, derived within the framework of meson theory or more recently in terms of chiral effective field theory, yield new possibilities for achieving a unified microscopic description of atomic nuclei. Based on spectral distribution methods, a comparison of these interactions to a most general $\mathrm{Sp}(4)$ dynamically symmetric interaction, which previously we found to reproduce well that part of the interaction that is responsible for shaping pairing-governed isobaric analog 0^+ states, can determine the extent to which this significantly simpler model Hamiltonian can be used to obtain an approximate, yet very good description of low-lying nuclear structure. And furthermore, one can apply this model in situations that would otherwise be prohibitive because of the size of the model space. In addition, we introduce a $\mathrm{Sp}(4)$ symmetry breaking term by including the quadrupole-quadrupole interaction in the analysis and examining the capacity of this extended model interaction to imitate realistic interactions. This provides a further step towards gaining a better understanding of the underlying foundation of realistic interactions and their ability to reproduce striking features of nuclei such as strong pairing correlations or collective rotational motion.

1 Introduction

Spectral distribution theory [1, 2] is an excellent framework for comparing the overall behavior of microscopic interactions and uncovering fundamental

properties of realistic NN potentials as well as derivative effective interactions [2, 3, 4]. Likewise, this information can be propagated beyond the defining two-nucleon system to nuclei with larger numbers of nucleons [2] and for higher values of isospin [5]. We search for the level of respect for selected underlying symmetries [6, 7] such as the $\mathrm{Sp}(4)$ symmetry [8, 9] of isovector (like-particle and proton-neutron, pn) pairing correlations plus an isoscalar pn force and the $\mathrm{SU}(3)$ symmetry [10] of collective rotational modes. Such symmetry-respecting microscopic model interactions can be used to probe the pairing and rotational characteristics of a realistic interaction [11, 12, 13, 14], which will reflect the characteristic properties of the pairing (quadrupole) model Hamiltonian if both interactions strongly correlate. As these symmetries are clearly important for certain spectral features (for example, observed pairing gaps and enhanced electric quadrupole transitions), we have a tool for rapidly assessing the likely success of these interactions for reproducing those spectral features.

Recent applications of the theory of spectral distributions also include quantum chaos, nuclear reactions and nuclear astrophysics with studies on nuclear level densities, transition strength densities, and parity/time-reversal violation (for example, see [15]). The significance of the method is related to the fact that low-order energy moments over a certain domain of single-particle states, such as the energy centroid of an interaction (its average expectation value) and the deviation from that average, yield valuable information about the interaction that is of fundamental importance [4, 12, 14, 16, 17, 18] without the need for carrying out large-dimensional matrix diagonalization and with little to no limitations due to the dimensionality of the vector space. Note that if one were to include higher-order energy moments, one would gradually obtain more detailed results that, in principle, would eventually reproduce those of a conventional microscopic calculations.

We compare three modern interactions, namely, the CD-Bonn [19], CD-Bonn+3terms [20] and GXPF1 [21], based on realistic nucleon-nucleon potentials, as well as two model interactions with pairing and quadrupole terms, which typically dominate in nuclei. CD-Bonn is a charge-dependent one-boson-exchange nucleon-nucleon (NN) potential that is one of the most accurate in reproducing the available proton-proton and neutron-proton scattering data. We employ the two-body matrix elements of the effective interaction derived from CD-Bonn for $0\hbar\omega$ no-core shell model (NCSM) calculations in the fp shell. In addition, the CD-Bonn+3terms interaction introduces phenomenological isospin-dependent central terms plus a tensor force with strengths and ranges determined in no-core $0\hbar\omega$ shell model calculations to achieve an improved description of the $A = 48$ Ca, Sc and Ti isobars. The GXPF1 effective interaction is obtained from a realistic G-matrix interaction based on the Bonn-C potential [22] by adding empirical corrections determined through systematic fitting to experimental energy data in the fp shell.

Several detailed reviews of the nuclear shell model and its applications have been published recently [23, 24, 25] that delve into related key physics issues

that we explore. However, the present study is novel and includes fp-shell interactions, which have been developed since those reviews were completed.

2 Theoretical Framework

The theory of spectral distributions (or statistical spectroscopy) is well documented in the literature [1, 2, 5, 16, 26, 27]. Spectral distribution theory combines important features, the most significant of which are as follows:

1. The theory provides a precise measure, namely, the correlation coefficient, for the overall similarity of two interactions. Literally the correlation coefficient is a measure of the extent to which two interactions "look like" (are correlated with) one another. In this respect, correlation coefficients can be used to extract information how well pairing/rotational features are developed in realistic interactions, which may differ substantially from an individual comparison of pairing/quadrupole interaction strengths [6].

2. It gives an exact prescription for identifying the *pure* zero- (centroid), one- and two-body parts of an interaction under a given space partitioning. Therefore, major properties follow:

   (a) The correlation coefficients are independent of the interaction centroids. (A direct comparison of two-body matrix elements provided by NN potentials may be misleading, especially when the averages of the interactions differ considerably.)

   (b) The pure one-body part of an interaction, the so-called induced single-particle energies, is naturally identified in the framework of spectral distribution theory and is indeed the average monopole interaction (compare to [21]). As such it influences the evolution of the shell structure, shell gaps and binding energies [28].

   (c) The pure two-body part is essential for studies of detailed property-defining two-body interactions beyond strong mean-field effects.

3. The correlation coefficient concept can be propagated straightforwardly beyond the defining two-nucleon system to derivative systems with larger numbers of nucleons [2] and higher values of isospin [5]. This, in addition to the two-nucleon information provided by alternative approaches (e.g.,[29]), yields valuable overall information, without a need for carrying out extensive shell-model calculations, about the universal properties of a two-body interaction in shaping many-particle nuclear systems.

For a scalar $\alpha = n$ (isospin-scalar $\alpha = n, T$) spectral distribution[1] the correlation coefficient between two Hamiltonian operators H and H' is defined as

$$\zeta^{\alpha}_{H,H'} = \frac{\langle (H^{\dagger} - \langle H^{\dagger} \rangle^{\alpha})(H' - \langle H' \rangle^{\alpha}) \rangle^{\alpha}}{\sigma_H \sigma_{H'}} = \frac{\langle H^{\dagger} H' \rangle^{\alpha} - \langle H^{\dagger} \rangle^{\alpha} \langle H' \rangle^{\alpha}}{\sigma_H \sigma_{H'}}, \quad (1)$$

where the "width" of H is the positive square root of the variance,

$$(\sigma^{\alpha}_{H})^2 = \langle (H - \langle H \rangle^{\alpha})^2 \rangle^{\alpha} = \langle H^2 \rangle^{\alpha} - (\langle H \rangle^{\alpha})^2, \quad (2)$$

and $\langle \cdots \rangle^{\alpha}$ denotes an average value related to the trace of an operator divided by the dimensionality of the space. The significance of a positive correlation coefficient is given by Cohen [30] and later revised to the following table:

Table 1. Interpretation of a correlation coefficient.

trivial	small	medium	large	very large	nearly perfect	perfect
0.00-0.09	0.10-0.29	0.30-0.49	0.50-0.69	0.70-0.89	0.90-0.99	1.00

From a geometrical perspective, in spectral distribution theory every interaction is associated with a vector and the correlation coefficient ζ (Eq. 1) defines the angle (via a normalized scalar product) between two vectors of length σ (Eq. 2). Hence, $\zeta_{H,H'}$ gives the normalized projection of H onto the H' interaction (or H' onto H). In addition, $(\zeta_{H,H'})^2$ gives the percentage of H that reflects the characteristic properties of the H' interaction.

3 Understanding the Nuclear Interaction in Many-nucleon Systems

We compare the three modern interactions, $H_0 = \{$CD-Bonn, CD-Bonn+3terms, GXPF1$\}$, based on realistic nucleon-nucleon potentials, and two model pairing and quadrupole isoscalar interactions in the fp region by means of the theory of spectral distributions. The first model interaction, $H_{\mathfrak{sp}(4)}$, is the most general $\mathrm{Sp}(4)$-dynamically symmetric interaction for a system of n valence nucleons in a 4Ω-dimensional space [8, 9] with two-body antisymmetric JT-coupled matrix elements for $\{r \leq (s,t);\ t \leq u\}$ orbits [6],

$$W^{JT}_{rstu} = -G_0 \frac{\sqrt{\Omega_r \Omega_t}}{\Omega} \delta_{(JT),(01)} \delta_{rs} \delta_{tu} - \{-E_0[(-)^T + \tfrac{1}{2}] + C\} \delta_{rt} \delta_{su}, \quad (3)$$

where $G_0 = G + \frac{F}{3}$, $E_0 = (\frac{E}{2\Omega} + \frac{D}{3})$, G, F, E, D and C are interaction strength parameters (see Table I in Ref.[9] for parameter estimates). The $\mathfrak{sp}(4)$ algebraic structure is exactly the one needed in nuclear isobaric analog 0^+ states to describe proton-proton (pp), neutron-neutron (nn) and proton-neutron

[1] For n particles distributed over 4Ω single-particle states, *scalar* (or *isospin-scalar*) distribution is called the spectral distribution averaged over the ensemble of all n-particle states (of isospin T) associated with the $\mathrm{U}(4\Omega)$ group structure (or $\mathrm{U}(2\Omega) \otimes \mathrm{U}(2)_T$).

(pn) isovector pairing correlations [the first term in (3)], while the second term includes isoscalar pn force related to the E_0 isospin symmetry term.

In addition, we construct an extended pairing plus quadrupole model, H_M, by including an additional traceless quadrupole-quadrupole interaction that being symmetric under $\mathrm{SU}(3)$ breaks the $\mathrm{Sp}(4)$ symmetry,

$$H_M = H_{\mathfrak{sp}(4)} + H_Q^{\perp}(2),\ H_Q = -\frac{\chi}{2} Q \cdot Q, \tag{4}$$

where χ is the only parameter in the present analysis and is determined by optimum correlation coefficients. The $H_Q^{\perp}(2)$-term is the part of the pure two-body $H_Q(2)$ interaction that is not contained in (is orthogonal to) the $\mathrm{Sp}(4)$ interaction[1]. This is because the $\mathrm{Sp}(4)$ interaction contains a nonnegligible part of the quadrupole-quadrupole interaction that is revealed by the correlation between H_Q and $H_{\mathfrak{sp}(4)}$. Namely, in the scalar case it is 15% ($1f_{7/2}$), 29% ($1f_{5/2}$) and 29% ($2p_{1/2}2p_{3/2}$), and for the T=1 part of the interactions in the isospin-scalar case, it is 34% ($1f_{7/2}$), 58% ($1f_{5/2}$) and 58% ($2p_{1/2}2p_{3/2}$). This is probably one of the reasons why the $\mathrm{Sp}(4)$ model interaction turns out to work rather well despite no explicit appearance of the quadrupole-quadrupole interaction.

The present study focuses on the weaker but property-defining two-body part of the interactions, such as $H_0(2)$, in the $1f_{7/2}$ [6] and upper *fp*-shell [7] domains. Such a partitioning of the fp oscillator shell follows naturally from a splitting of these two regions by a strong spin-orbit interaction. Several correlation coefficients are of particular interest. Specifically, the overall similarity between a realistic interaction and the extended pairing+quadrupole model interaction in the (isospin-) scalar case is estimated by the $\zeta^{n(T)}_{H_0(2),H_M}$ correlation, while the capability of a realistic interaction to describe rotational collective motion, and hence to reproduce rotational bands and enhanced electric quadrupole transitions, can be detected via its correlation to the full $H_Q(2)$ quadrupole-quadrupole two-body interaction, $\zeta^{n(T)}_{H_0(2),H_Q(2)}$. The isospin-scalar space partitioning is where the ability of a realistic interaction to form correlated pairs and hence reproduce prominent pairing gaps is detected via $\zeta^{n,T}_{H_0(2),H_{\mathfrak{sp}(4)}}$. In the present analysis, the $\zeta^{n(T)}_{H_0(2),H_Q(2)}$ and $\zeta^{n,T}_{H_0(2),H_{\mathfrak{sp}(4)}}$ correlation coefficients are independent of the quadrupole/pairing interaction strength parameters.

In the detailed case of isospin-scalar distribution in the $1f_{7/2}$ orbit, the CD-Bonn, CD-Bonn+3terms and GXPF1 interactions are found to contain on average 59%, 77%, and 78%, respectively, of the pairing+quadrupole interaction. This percentage goes up to 91%, 97%, and 92%, respectively, for the highest possible isospin group of states for all the nuclei with valence protons and neutrons occupying the $1f_{7/2}$ shell (Fig. 1). For these states, the strongest correlation was observed between the CD-Bonn+3terms and the pairing+quadrupole

[1] Such a Hamiltonian (Eq. 4) does not affect the centroid of $H_{\mathfrak{sp}(4)}$ because $H_Q^{\perp}(2)$ is traceless and hence preserves the shell structure that is built into $H_{\mathfrak{sp}(4)}$ and established by a harmonic oscillator potential and as a result is favored in many studies [12, 14, 31].

model interaction, where other types of interactions accounted for in the realistic interaction represent only 3% of it. They constitute 8% of the GXPF1 interaction, and 9% of CD-Bonn. While both interactions, CD-Bonn+3terms and GXPF1, exhibit a well-developed pairing character compared to CD-Bonn, the latter appears to build up more (less) rotational collective features that are outside of the scope of the $T = 1$ ($T = 0$) $\mathrm{Sp}(4)$ interaction.

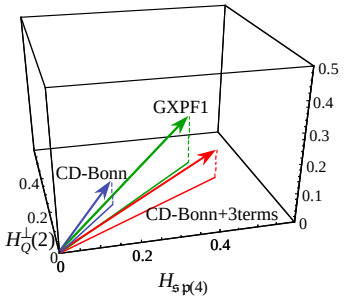

Figure 1. Geometrical representation of the $T = 1$ CD-Bonn (light blue), CD-Bonn+3terms (red) and GXPF1 (green) interactions, in an abstract operator space, where the horizontal plane is spanned by the orthogonal linear operators, the pure two-body $H_{\mathfrak{sp}(4)}$ and $H_Q^{\perp}(2)$ model Hamiltonians, both linearly independent of the residual interaction operators represented by the vertical axis. The orientation of the vectors remains the same for any particle number $n \geq 2$ and for all $T = n/2$ cases.

The abovementioned strong correlation coefficients, $\zeta_{H_0,H_M}^{n,T=n/2}$, imply that both realistic and H_M interactions are expected to yield energy spectra of a similar pattern. Indeed, for these cases the pairing+quadrupole model interaction appears to be a very good approximation that provides a reasonable description of the energy spectra of the nuclei in the $1f_{7/2}$ level (Fig. 2).

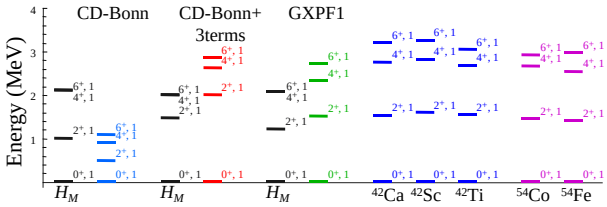

Figure 2. Energy spectra of $T = 1$ states predicted by the CD-Bonn (light blue), CD-Bonn+3terms (red) and GXPF1 (green) interactions. Each is compared to the model Hamiltonian H_M (black) with $\chi = 0.071,\ 0.036$ and 0.055, respectively. For comparison, the experimental $T = 1$ energy spectra of the $A = 42$ Ca, Sc, Ti isobars (blue) and $A = 54$ Co and Fe isobars (magenta) are also shown.

In the upper *fp* domain the outcome yields strong correlation of the pure

two-body GXPF1 interaction with the pairing+quadrupole extended model in both scalar and isospin-scalar distributions (Fig. 3). Particularly, the outcomes

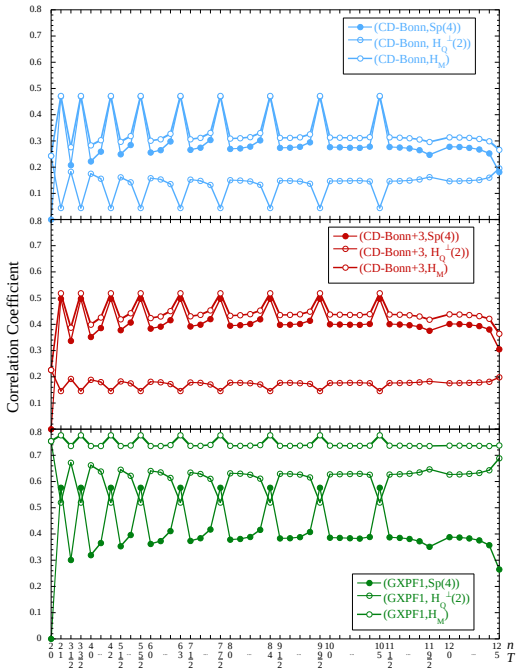

Figure 3. Correlation coefficients of the pure two-body CD-Bonn (blue), CD-Bonn+3terms (red) and GXPF1 (green) interactions with $H_{\mathfrak{sp}(4)}$ (filled symbols), $H_Q^{\perp}(2)$ (transparent symbols) and H_M (empty symbols) in the upper *fp* shell for the isospin-scalar distribution. For each valence particle number, n, the isospin T varies as $\frac{n}{2}, \frac{n}{2}-1, \ldots, 0(\frac{1}{2})$. The figures are symmetric with respect to the sign of $n-2\Omega$.

show very good scalar-distribution correlations of GXPF1 with the $\mathrm{Sp}(4)$ dynamically symmetric interaction and with the $H_Q(2)$ quadrupole-quadrupole interaction (Table 2). Rotational features within many-nucleon systems in the upper *fp* domain are found to be more fully developed for GXPF1 and less for CD-Bonn+3terms and CD-Bonn. The isospin-scalar space partitioning demonstrates a tendency in GXPF1 towards the formation of correlated pairs in the highest possible isospin groups of states (Fig. 3).

The different extent to which the GXPF1 interaction compared to the CD-Bonn and CD-Bonn+3terms interactions reflects development of pairing correlations and collective rotational modes in the upper *fp* domain may be the reason why their pure two-body part do not correlate as strongly as, for example, CD-Bonn and CD-Bonn+3terms do. Namely, in the scalar case the pure two-body correlations are 0.90 (between CD-Bonn and CD-Bonn+3terms) and only 0.56 (CD-Bonn and GXPF1) and 0.53 (CD-Bonn+3terms and GXPF1).

Table 2. Correlation coefficients for many-nucleon systems of the $H_0(2)$ pure two-body part of the CD-Bonn, CD-Bonn+3terms and GXPF1 interactions with $H_{\mathfrak{sp}(4)}$ and $H_Q^{\perp}(2)$, with the pure two-body full quadrupole-quadrupole interaction, $H_Q(2)$, and with the extended pairing+quadrupole model interaction H_M (Eq. 4).

	CD-Bonn	CD-Bonn+3terms	GXPF1
$\zeta_{H_0(2),H_{\mathfrak{sp}(4)}}$	0.55	0.50	0.65
$\zeta_{H_0(2),H_Q^{\perp}(2)}$	0.14	0.20	0.51
$\zeta_{H_0(2),H_Q(2)}$	0.28	0.33	0.67
$\zeta_{H_0(2),H_M}$	0.57	0.54	0.83

In the isospin-scalar case, the correlations vary slightly with the particle number and isospin and they are on average, 0.88 (between CD-Bonn and CD-Bonn+3terms), 0.40 (CD-Bonn and GXPF1), and 0.37 (CD-Bonn+3terms and GXPF1). In addition, one can compare the significant monopole influence of the three interactions, which is very similar for all when averaged over the isospin values. However, in the isospin-scalar distribution, the correlation coefficients involving the induced effective one-body contribution differ between GXPF1 and the two CD-Bonn interactions. Their behavior, especially below mid-shell, reflects the similarity of the corresponding $T = 0$ induced single-particle energies and the opposite signs of the corresponding $\lambda_{3/2}^{T=1}$ (for $2p_{3/2}$) and $\lambda_{5/2}^{T=1}$ (for $1f_{5/2}$) pure one-body interactions.

Individual orbit analysis, including the $1f_{7/2}$, $1f_{5/2}$, $2p_{1/2}$, and $2p_{3/2}$ levels, shows considerably stronger correlation of all the interactions with the pairing+quadrupole model interaction (up to $0.8-1.00$) as well as in nuclear systems with more than two nucleons. However, more prominent differences among the interactions appear in the multi-j upper *fp* domain especially concerning both CD-Bonn interactions. This may indicate that the inter-orbit interactions do not respect strongly the symmetries imposed in the model interactions. In addition, the interaction strengths may differ from one orbit to another. While they do not affect correlation coefficients in the singe-j cases, their relative strength is of a great importance for multi-j analysis. In addition, the difference in the behavior of CD-Bonn+3terms within both regions, $1f_{7/2}$ and upper *fp*, may reflect the fact that this interaction was determined through a reproduction of the energy spectrum and binding energy of $A = 48$ $1f_{7/2}$ nuclei.

In the upper *fp* region, the extended H_M pairing+quadrupole interaction is strongly correlated with the pure two-body GXPF1 interaction especially in the scalar distribution (Table 2) and for this reason can be used as a good approximation. This is reflected in the quite good agreement between the experimental low-lying energy spectra of ^{58}Ni and ^{58}Cu and the theoretical prediction based on the H_M model interaction with $\chi = 0.027$ (see Eq. 4) in the $1f_{5/2}2p_{1/2}2p_{3/2}1g_{9/2}$ major shell (Fig. 4).

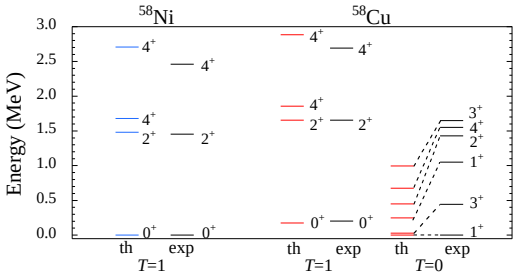

Figure 4. Theoretical ('th') low-lying energy spectra for ^{58}Ni (left, blue) and ^{58}Cu (right, red) compared to experiment ('exp', black). The theoretical calculations are performed in the $1f_{5/2}2p_{1/2}2p_{3/2}1g_{9/2}$ major shell with the H_M model interaction with $\chi = 0.027$ and with single-particle energies derived from ^{57}Ni experimental energy levels.

In summary, the present study reveals important information, within the framework of spectral distribution theory, about the types of forces that dominate the fp-shell CD-Bonn, CD-Bonn+3terms and GXPF1 interactions in nuclei and their ability to account for many-particle effects such as the formation of correlated nucleon pairs and enhanced quadrupole collective modes. The results also illustrate that interactions, which were found to strongly correlate, produced energy spectra of a similar pattern.

Acknowledgments

JPV would like to thank Sorina Popescu, Sabin Stoica and Geanina Negoita for valuable discussions. This work was supported by the US National Science Foundation, Grant Numbers 0140300 & 0500291, and the Southeastern Universities Research Association, as well as partly performed under the auspices of the US Department of Energy by the University of California, Lawrence Livermore National Laboratory under contract No. W-7405-Eng-48 and under the auspices of grants DE-FG02-87ER40371 & DE–AC02–76SF00515.

References

[1] J. B. French and K. F. Ratcliff, *Phys. Rev.* **C3**, 94 (1971).

[2] F. S. Chang, J. B. French, and T. H. Thio, *Ann. Phys.* (N.Y.) **66**, 137 (1971).

[3] J. P. Draayer, J. B. French, V. Potbhare, and S. S. M. Wong, *Phys. Lett.* **55B**, 263, 349 (1975); B. D. Chang and J. P. Draayer, *Phys. Rev.* **C20**, 2387 (1979).

[4] V. Potbhare, *Nucl. Phys.* **A289**, 373 (1977).

[5] K. T. Hecht and J. P. Draayer, *Nucl. Phys.* **A223**, 285 (1974).

[6] K. D. Sviratcheva, J. P. Draayer, and J. P. Vary, *Phys. Rev.* **C73**, 034324 (2006).

[7] K. D. Sviratcheva, J. P. Draayer, and J. P. Vary, submitted (2006).

[8] K. D. Sviratcheva, A. I. Georgieva, and J. P. Draayer, Phys. Rev. **C69** 024313 (2004).

[9] K. D. Sviratcheva, A. I. Georgieva, and J. P. Draayer, Phys. Rev. **C70** 064302 (2004).
[10] J. P. Elliott, *Proc. Roy. Soc.* (London) **A245**, 128 (1958); **A245**, 562 (1958); J. P. Elliott and M. Harvey, *Proc. Roy. Soc.* (London) **A272**, 557 (1963).
[11] J. P. Draayer, *Nucl. Phys.* **A216**, 457 (1973).
[12] T. R. Halemane, K. Kar, and J. P. Draayer, *Nucl. Phys.* **A311**, 301 (1978).
[13] V. K. B. Kota, S. P. Pandya, and V. Potbhare, *Nucl. Phys.* **A349**, 397 (1980).
[14] C. R. Countee, J. P. Draayer, T. R. Halemane, and K. Kar, *Nucl. Phys.* **A356**, 1 (1981).
[15] J. B. French, V. K. B. Kota, A. Pandey, and S. Tomsovic, Ann. Phys. (N.Y.) **181**, 235 (1988); V. K. B. Kota and D. Majumdar, Z. Phys. A **351**, 365 (1995); Z. Phys. A **351**, 377 (1995); S. Tomsovic, M. B. Johnson, A. Hayes, and J. D. Bowman, *Phys. Rev.* **C62**, 054607 (2000); J. M. G. Gomez, K. Kar, V. K. B. Kota, R. A. Molina, and J. Retamosa, *Phys. Lett.* **B 567**, 251 (2003); M. Horoi, M. Ghita, and V. Zelevinsky, *Phys. Rev.* **C69**, 041307(R) (2004); N. D. Chavda, V. Potbhare, and V. K. B. Kota, *Phys. Lett.*, **A 326**, 47 (2004); V. K. B. Kota, *Phys. Rev.* **C71**, 041304(R) (2005); Y. M. Zhao, A. Arima, N. Yoshida, K. Ogawa, N. Yoshinaga, and V. K. B. Kota, *Phys. Rev.* **C72**, 064314 (2005).
[16] J. B. French, in *Dynamic Structure of Nuclear States*, ed. D. J. Rowe *et al.* (Univ. of Toronto Press, Toronto, 1972), p.154.
[17] J. P. Draayer and G. Rosensteel *Phys. Lett.* **124B**, 281 (1983); G. Rosensteel and J. P. Draayer, *Nucl. Phys.* **A436**, 445 (1985).
[18] K. F. Ratcliff, *Phys. Rev.* **C3**, 117 (1971); B. J. Dalton, W. J. Baldridge, and J. P. Vary, *Phys. Rev.* **C20**, 1908 (1979); S. Sarkar, K. Kar, and V. K. B. Kota, *Phys. Rev.* **C36**, 2700 (1987).
[19] R. Machleidt, F. Sammarruca, and Y. Song, *Phys. Rev.* **C53**, R1483 (1996); R. Machleidt, *Phys. Rev.* **C63**, 024001 (2001).
[20] S. Popescu, S. Stoica, J. P. Vary, and P. Navratil, to be published.
[21] M. Honma, T. Otsuka, B. A. Brown, and T. Mizusaki, *Phys. Rev.* **C69**, 034335 (2004).
[22] M. Hjorth-Jensen, T. T. S. Kuo, and E. Osnes, *Phys. Rep.* **261**, 125 (1995).
[23] E. Caurier, G. Martinez-Pinedo, F. Nowacki, A. Poves, and A. P. Zuker, *Rev. Mod. Phys.* **77**, 427 (2005).
[24] B. A. Brown, *Prog. Part. Nucl. Phys.* **47**, 517 (2001).
[25] T. Otsuka, M. Honma, T. Mizusaki, N. Shimizu, and Y. Utsuno, *Prog. Part. Nucl. Phys.* **47**, 319 (2001).
[26] V. K. B. Kota, *Phys. Rev.* **C20**, 347 (1979); Fortran Programs for Statistical Spectroscopy Calculations.
[27] B. D. Chang, J. P. Draayer, and S. S. M. Wong, *Comput. Phys. Commun.* **28**, 41 (1982).
[28] T. Otsuka *et al.*, *Phys. Rev. Lett.* **87**, 082502 (2001).
[29] M. Dufour and A. P. Zuker, *Phys. Rev.* **C54**, 1641 (1996).
[30] J. Cohen, *Statistical Power Analysis for the Behavioral Sciences* (Lawrence Erlbaum Associates, Hillsdale, New Jersey, 1988); J. Cohen, P. Cohen, S. G. West, and L. S. Aiken, *Applied multiple regression/correlation analysis for the behavioral sciences*, 2nd ed. (Lawrence Erlbaum Associates, Hillsdale, New Jersey, 2003).
[31] J. P. Draayer and G. Rosensteel, *Phys. Lett.* **125B**, 237 (1983).